Ca^{2+}-Induced Lateral Phase Separation in Phosphatidic Acid/Phosphatidylcholine Monolayers As Revealed by Fluorescence Microscopy†

Kari K. Eklund,‡ Jorma Vuorinen, Jukka Mikkola, Jorma A. Virtanen, and Paavo K. J. Kinnunen*
Department of Membrane Physics, KSV Research Laboratories, P.O. Box 128, SF-00381 Helsinki, Finland
Received September 1, 1987; Revised Manuscript Received December 16, 1987

ABSTRACT: Phase separation in mixed monolayers of phosphatidylcholine (PC) and pyrene-labeled phosphatidic acid (PA) was observed by fluorescence microscopy on an air/water interface as a function of subphase Ca^{2+} concentration and lateral packing pressure of the film. Below 45 mN m^{-1} and in the absence of Ca^{2+} no indications of phase immiscibility were observed. Addition of 1 mM Ca^{2+} caused extensive phase separation, which was evident immediately after spreading of the film. Further increase in Ca^{2+} concentration up to 30 mM increased the pyrene excimer intensity of the separated phosphatidic acid enriched domains. In the presence of Ca^{2+} (1–30 mM) and at surface pressures below 10 mN m^{-1} phase separation was always evident. However, as surface pressure exceeded 10 mN m^{-1}, mixing of PC and PA occurred. Upon decompression of the film, phase separation reappeared at surface pressures close to 10 mN m^{-1}. The surface textures of the film before and after the compression and subsequent relaxation were different. Inclusion of 30 mol % cholesterol increased the number and decreased the size of the PA domains. In films containing 50 mol % cholesterol no phase separation could be detected at the resolution available.

Lateral phase separation of membrane phospholipids can induce profound changes in membrane functions, such as activation of membrane enzymes (Sandermann et al., 1978; Robinson et al., 1982), and changes in electrical properties. In model biomembranes phase separation has been shown to lead to enhanced permeability (Linden et al., 1973; Papahadjopoulos et al., 1973; Marsh et al., 1976), reorganization of membrane components (Kleeman et al., 1976), binding of a peripheral membrane protein, cytochrome *c* (Mustonen et al., 1987), and fusion of phospholipid vesicles (Papahadjopoulos et al., 1976; Silvius et al., 1984; Leventis et al., 1986). In order to understand the physiological significance of phase separation, it is relevant to study the circumstances and mechanisms that lead into isothermal phase separation processes between different phospholipid species.

Addition of Ca^{2+} ions causes extensive phase separation of certain negatively charged and neutral phospholipids. Most thoroughly studied is Ca^{2+}-induced phase separation in PS/PC (Jacobson et al., 1975; van Dijck et al., 1978; Parente et al., 1986; Ito et al., 1974) and PA/PC membrane alloys (Galla et al., 1975; Graham et al., 1985; Kouaouci et al., 1985). Phase separation between neutral and negatively charged phospholipids can also be induced by positively charged proteins such as cytochrome *c* (Birrell et al., 1976; Mustonen et al., 1987) or polylysine (Gad et al., 1982; Gad, 1983).

In fluorescence spectroscopy the use of fluorophores containing the label covalently attached to a phospholipid has recently gained increasing interest. Due to their versatile spectroscopic properties pyrene-labeled phospholipid analogues are widely used and are perhaps the most thoroughly characterized membrane probes. The features of fluorescence emission of pyrene depend on the local concentration of the probe and lipid diffusion rates (Förster et al., 1969; Galla et al., 1980). Therefore, fluorescence spectroscopic data provide information on phospholipid phase transitions and lateral diffusion, packing, and distribution of pyrene-labeled phospholipids (Galla et al., 1980; Somerharju et al., 1985; Thuren et al., 1984, 1986; Kinnunen et al., 1986, 1987; Hresko et al., 1986, 1987). Although the presence of pyrene in the fatty acid of a phospholipid does to some extent perturb the hydrocarbon part of the membrane, this perturbation does not mask head group dependent interactions between phospholipids (Somerharju et al., 1985; Thuren et al., 1986; Kinnunen et al., 1986).

Recently fluorescence microscopy and digital image processing have been introduced to study the behavior of phospholipid monolayers and very recently also liposomes. Novel and highly informative data concerning phase separations and transitions have been obtained (Peters & Beck, 1983; Lösche & Möhwald, 1984a,b; McConnell et al., 1984; Weis & McConnell, 1984; Haverstick & Glaser, 1987). The present study demonstrates lateral distribution in a film of two different phospholipid species, DPPC and PPHPA, and describes the effects of Ca^{2+}, cholesterol, and lateral surface pressure.

Materials and Methods

1,2-Dipalmitoyl-*sn*-glycero-3-phosphatidylcholine (DPPC)[1] was from Sigma. The ammonium salt of 1-palmitoyl-2-[6-(pyren-1-yl)hexanoyl]-*sn*-glycero-3-phospatidic acid (PPHPA), shown in Figure 1, was obtained from KSV Chemical Corp. (Helsinki, Finland). No impurities were detected in these lipids upon thin-layer chromatography on silica gel (Merck, Darmstadt, West Germany), and they were used without further purification. Other chemicals were of reagent grade. Water was freshly deionized and purified in a Milli-RO/Milli-Q (Millipore) filtering system. All experiments were conducted in a clean room at a temperature of 22 °C.

Lipids were mixed in chloroform in the indicated molar ratios and were subsequently spread from this solvent to form monolayers. The subphase was a 100 mM NaCl and 20 mM Tris-HCl, pH 7.4, buffer with the indicated concentrations of

† This work was supported by a grant (to K.K.E.) from the Magnus Ehrnrooth Foundation.
* Address correspondence to this author.
‡ Permanent address: Department of Medical Chemistry, University of Helsinki, Siltavuorenpenger 10, SF-00170 Helsinki, Finland.

[1] Abbreviations: DPPC, 1,2-dipalmitoyl-*sn*-glycero-3-phosphatidylcholine; PPHPA, 1-palmitoyl-2-[6-(pyren-1-yl)hexanoyl]-*sn*-glycero-3-phosphatidic acid; Tris, tris(hydroxymethyl)aminomethane; EDTA, ethylenediaminetetraacetic acid; PS, phosphatidylserine; PE, phosphatidylethanolamine.

0006-2960/88/0427-3433$01.50/0

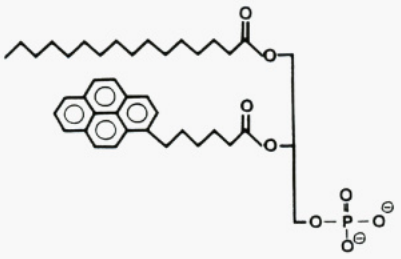

FIGURE 1: Molecular structure of PPHPA.

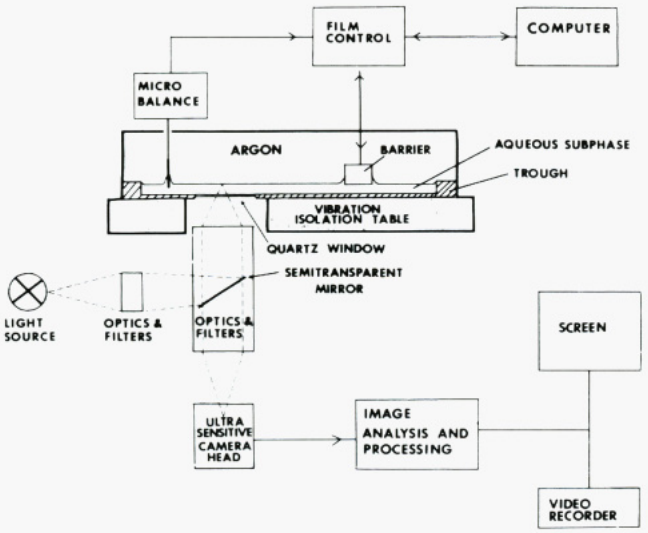

FIGURE 2: Block diagram of the instrumental setup.

calcium chloride. In the absence of Ca^{2+} 1.0 mM EDTA was included. Surface pressure was recorded with a KSV-2200 DFC unit (KSV Chemical Corp.) connected to a Sperry PC. Before the compression the monolayer was allowed to settle for 1 h. The rate of the barrier movement during compression and relaxation did not exceed 1.9 Å molecule^{-1} min^{-1} (5 mm/min). The monolayer trough was enclosed in a gastight chamber filled with argon.

The construction of the equipment is schematically shown in Figure 2. The monolayer is viewed through a quartz window in the bottom of the Teflon trough. The film is illuminated through an Ealing (36×) reflective objective and the fluorescence image monitored through the same objective focused by a DC motor. The light source is a 200-W Hg lamp (Oriel). The excitation light was carried by a quartz fiber bundle and via a semitransparent mirror to the objective. The pyrene-labeled lipid probe has absorption maxima at 279, 330, and 343 nm. Accordingly, the excitation beam was obtained through a Schott UG 11 filter transmitting in the range 270–360 nm. Scattered stray light was reduced with adjustable irises. Fluorescence emission due to pyrene excimer at 470 nm was selected by 390-, 418-, and 425-nm cutoff filters and a red blocking filter (Schott BG 39). The image was collected into a Hamamatsu C1966-20 camera head, operated in the analog mode due to the high intensity of pyrene fluorescence emission. The signal was fed into a C1966 image analysis system. The images were stored with a Sony U-Matic VO 5630 video recorder continuously during compression or relaxation of the monolayer and were later replayed and photographed from the display screen. The images are shown in pseudocolors (0–255, eight levels) with the lowest intensity in the scale (blue) on the left. Two consecutive images were averaged to improve the still pictures, and the bit select was adjusted accordingly to "6–13". No other processing of the images was conducted. The background fluorescence in the

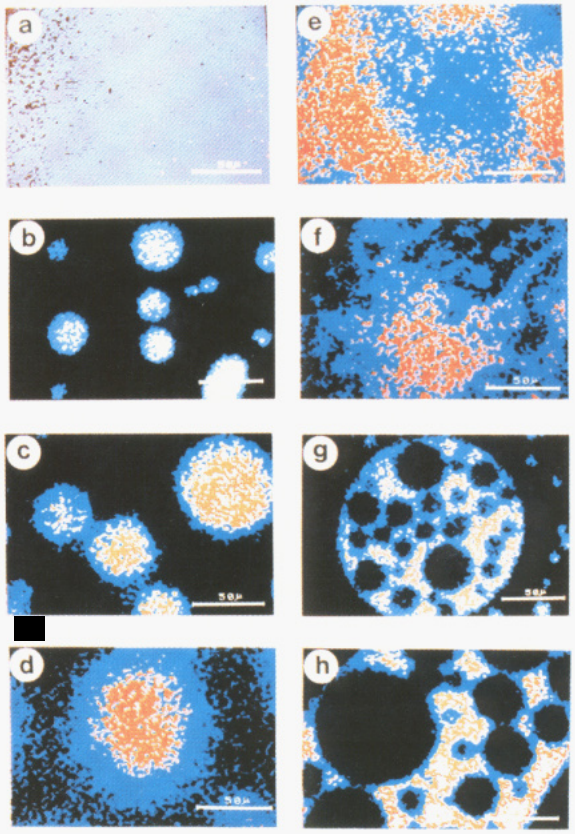

FIGURE 3: Textures in a mixed DPPC/PPHPA (80:20) film (a) in the absence of Ca^{2+} and (b–g) with 1 mM Ca^{2+} in the subphase. Surface pressure is (a) 1.0 mN m^{-1}, (b) 0.5 mN m^{-1}, (c) 5 mN m^{-1}, (d) 15 mN m^{-1}, and (e) 40 mN m^{-1}. Surface pressures during decompression of the same film are (f) 9.0 mN m^{-1}, (g) 2.0 mN m^{-1}, and (h) 0.3 mN m^{-1}.

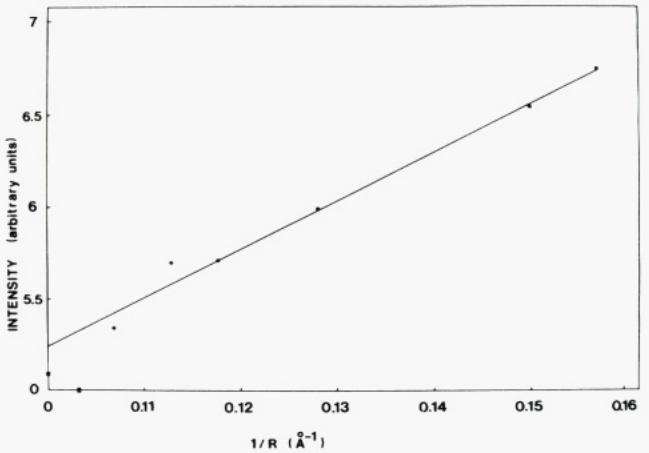

FIGURE 4: Pyrene excimer fluorescence intensity of a DPPC/PPHPA (80:20) film in the absence of Ca^{2+} as a function of the reciprocal of the calculated average distance between the pyrene moieties.

absence of pyrene was negligible and was therefore not subtracted. The lowest level of the labeled monolayer was adjusted to black, and the sensitivity settings of the system were thereafter kept constant. However, due to the extreme sensitivity of pyrene fluorescence to oxygen quenching, caution should be taken when considering the absolute intensities of the images. The images shown are considered to be representative of the entire monolayer.

RESULTS

Figure 3a shows a DPPC/PPHPA (80:20) monolayer on buffer at 1.0 mN m^{-1}. Uniform fluorescence intensity is ob-

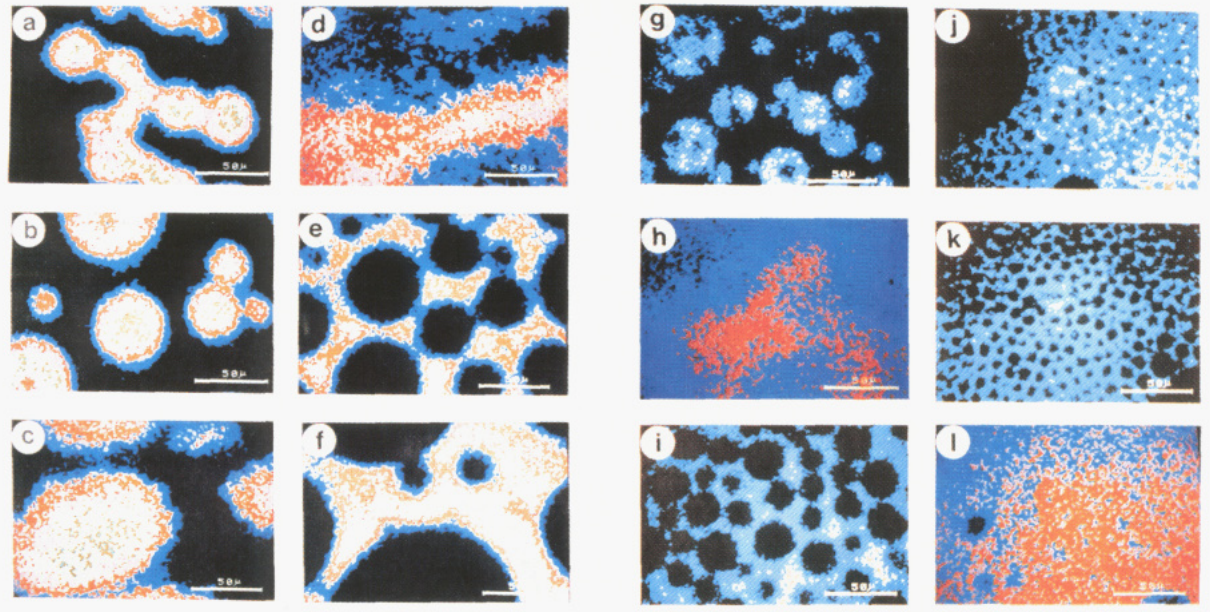

FIGURE 5: DPPC/PPHPA (80:20) monolayer over a subphase containing 30 mM Ca^{2+} concentration (a–f) and in the presence of varying concentrations of cholesterol over 5 mM Ca^{2+} (g–l). Surfaces pressures upon compression were (a) 0.5 mN m^{-1}, (b) 3 mN m^{-1}, (c) 9 mN m^{-1}, and (d) 40 mN m^{-1}. During decompressions images were obtained at (e) 3 mN m^{-1} and (f) 0.5 mN m^{-1}. In panels g–i 10 mol % cholesterol was included. Surface pressures are (g) 0.5 mN m^{-1}, (h) 10 mN m^{-1}, and after decompression (i) 0.5 mN m^{-1}. Cholesterol content in (j–l) is 30 mol % at surface pressures of (j) 0.5 mN m^{-1} and (k) 0.5 mN m^{-1} after decompression. In (l) 50 mol % cholesterol is present, and the surface pressure is 2.5 mN m^{-1}.

served, indicating that DPPC and PPHPA are readily miscible at this resolution. In the absence of calcium no indications of phase separation were revealed by microscopy at surface pressures below 45 mN m^{-1}. Upon compression of the film from 0 to 40 mN m^{-1} the total excimer fluorescence intensity increases monotonically. When these data were converted to show excimer fluorescence intensity versus reciprocal of the average distance between the fluorophores (assuming an even distribution of PPHPA in the film), a linear correlation was evident with a correlation coefficient of 0.993 by linear least-squares analysis (Figure 4). This is in accordance with our previous results on liposomes and Langmuir–Blodgett films (Thuren et al., 1986; Kinnunen et al., 1987). Figure 3b–e shows a PC/PA (80:20) film at different surface pressures over a subphase containing 1 mM Ca^{2+}. Figure 3b shows the film after a 1-h incubation at 0.5 mN m^{-1}. Clear phase separation between DPPC and the fluorescent PPHPA is evident with sharp phase boundaries. Fairly uniform size distribution (10–40-μm diameter) of the separated PA domains can be observed. The total area of the fluorescent PA corresponds to approximately 20% of the total area of the lipid monolayer.

As the surface pressure is increased further, the average size of the fluorescent domains gradually increases (Figure 3c) and clearly exceeds 20%, indicating the presence of a mixed DPPC/PPHPA phase. The phase boundaries between PC and PA become blurred close to 9 mN m^{-1} and indistinct at 15 mN m^{-1} (Figure 3d), with further increase in the size of the fluorescent domains. At higher surface pressures no clear phase boundaries between PC and PA can be observed (Figure 3e) although the intensity distribution is not as homogeneous as in the absence of Ca^{2+}. The images recorded during the decompression of the same film from 40 to 0 mN m^{-1} are shown in Figure 3f–h. At a surface pressure close to 9 mN m^{-1} dark areas of DPPC appear (Figure 3f). At 5 mN m^{-1} and at lower surface pressures clear phase separation is evident. However, the textures observed are different from those during compression of the film. First, the areas of PA are on the average larger (fewer in number), and there is DPPC accommodated in a nearly hexagonal order in the PA domains (Figure 3g). Second, in the same monolayer there are large areas in which DPPC forms round separated phases with PA squeezed in between as is illustrated in Figure 3h. During a 2-h observation period both of these structures are stable although there is some tendency of the separated PC areas to fuse into larger domains in a PA matrix (see, for instance, Figure 3h). During a repeated compression of the same monolayer the separate phases disappear when a surface pressure of 10 mN m^{-1} is approached. Upon subsequent relaxation structures identical with those in Figure 3f–h reappear (data not shown). Highest pyrene excimer fluorescence intensity is observed in the middle of the PA domains, thus indicating that near the phase boundaries some DPPC is accommodated in the fluorescent PA enriched areas.

In Figure 5a–f a DPPC/PPHPA (80:20) film is shown over a subphase containing 30 mM Ca^{2+}. Pyrene excimer intensity after the spreading of the film is higher than at 1 mM Ca^{2+}, and a strong tendency of the PA domains to stick together at pressures close to 0 mN m^{-1} can be observed (Figure 5a). As the film is compressed, blurring of the phase boundaries with a concomitant increase in the size of the PA domains is observed (Figure 5b,c) similarly to the films on 1 mM Ca^{2+}. However, even at high surface pressures mixing of PC and PA is incomplete (Figure 5d). Upon decompression structures similar to those observed on 1 mM Ca^{2+} can be seen (Figure 5e,f). Over 5 mM Ca^{2+} the surface textures upon compression and relaxation of the film were more like those observed at 1 mM Ca^{2+} and over 10 mM Ca^{2+} more similar to those surface textures observed at 30 mM Ca^{2+} (data not shown).

The effect of cholesterol on the phase separation in PC/PA films was also studied (Figure 5g–l). Low cholesterol concentrations (2–5 mol %) had no observable effect (data not shown). Upon inclusion of 10 mol % cholesterol some nonfluorescent spots can be observed in the PA domains after spreading of the film (Figure 5g). In addition, phase separation between PC and PA disappears at somewhat lower surface pressures (at 7 mN m^{-1}) than in the absence of cholesterol (Figure 5h). The surface textures observed after decompression consist of an increased number of PC domains

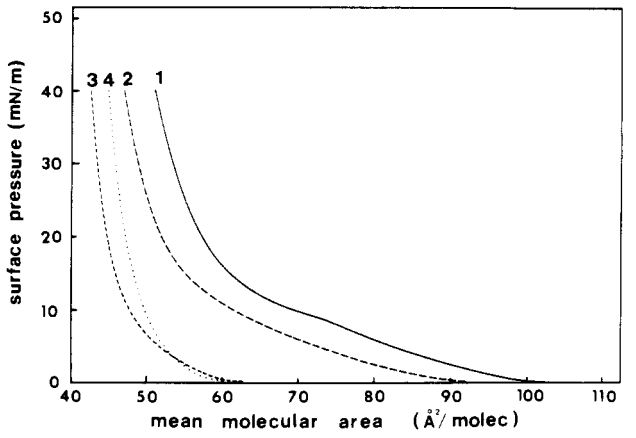

FIGURE 6: Compression isotherms of a DPPC/PPHPA (80:20) film over 5 mM Ca^{2+} in the presence of varying amounts of cholesterol: (1) no cholesterol and (2) 10 mol %, (3) 30 mol %, and (4) 50 mol % cholesterol.

of a decreased size in a PA matrix (Figure 5i), compared to texture present in the absence of cholesterol. In the presence of 30 mol % cholesterol the mean size of the DPPC domains decreases with only a few larger DPPC areas being present (Figure 5j). Homogeneous size distribution of 5–10 μm of the PC areas and nearly hexagonal ordering are seen after decompression (Figure 5k). In the presence of 50 mol % cholesterol no clear phase separation except for occasional seggregations of DPPC (Figure 5l) can be detected at the resolution available. The compression isotherms of DPPC/PPHPA/cholesterol film at varying cholesterol content are shown in Figure 6. Strong condensation of the film is evident up to 30 mol % cholesterol.

The compression isotherms of the DPPC/PPHPA (80:20) mixed film at varying subphase Ca^{2+} concentrations are shown in Figure 7a. Condensation of the film is evident up to 10 mM Ca^{2+} concentration. At 30 mM Ca^{2+} an increase in the mean molecular area is observed. This is further illustrated in Figure 7b, which shows the dependency of the area per molecule as a function of Ca^{2+} concentration at different surface pressures. A phase transition appears at 1 mM Ca^{2+} at 9 mN m^{-1} and becomes pronounced at 10 mM Ca^{2+}. In addition, a hysteresis during the compression–relaxation cycle of the mixed monolayer is evident. The area per molecule before the compression is smaller than after the decompression of the monolayer (Figure 8). During a 1-h incubation following the relaxation of the film the mean molecular area increases and returns to the value observed prior to compression (data not shown).

Discussion

Binary mixtures of DPPC and the negatively charged fluorescent PPHPA were studied. Some perturbation of the monolayer by the pyrene label is to be expected. However, it has been shown that the presence of pyrene in the fatty acid of phospholipid does not mask head group dependent interactions (Somerharju et al., 1985). Furthermore, the electrostatic binding of Ca^{2+} to PA is of high affinity.

In the absence of Ca^{2+} no phase separation between DPPC and PPHPA could be observed. This is in accordance with several other studies on PC/PA mixed membranes (Graham et al., 1985; Kouaouci et al., 1985). In the presence of 1 mM Ca^{2+} in the subphase immediate phase separation between PC and PA was observed after the spreading of the monolayer. This is in accordance with the fast kinetics (in seconds) of the calcium-induced lateral phase separation observed in mixed PC/PA liposomes (Graham et al., 1985).

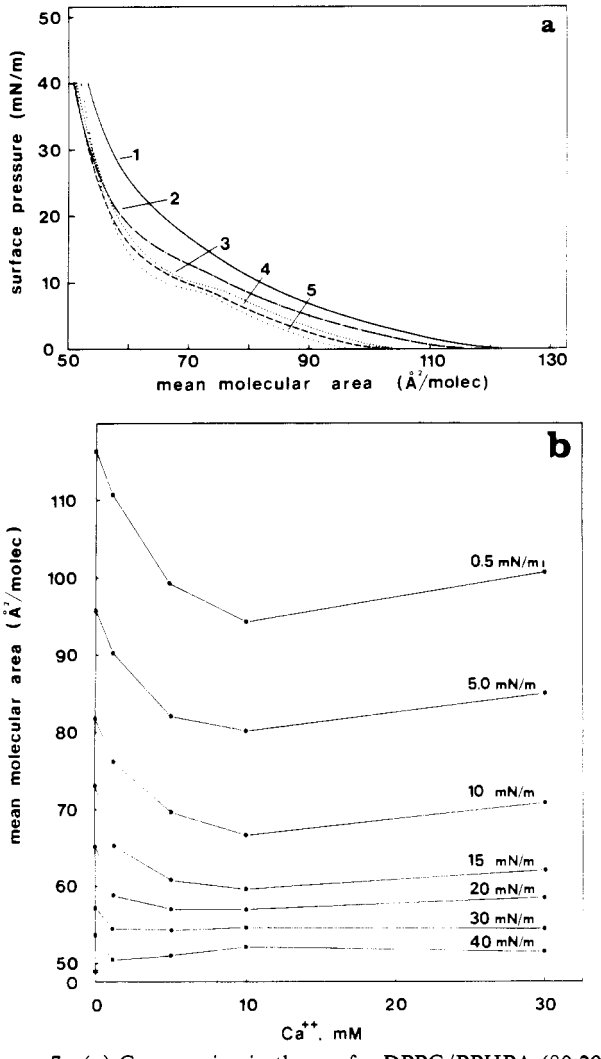

FIGURE 7: (a) Compression isotherms for DPPC/PPHPA (80:20) mixed monolayers in the presence of varying Ca^{2+} concentrations: (1) 0, (2) 1 mM, (3) 5 mM, (4) 10 mM, and (5) 30 mM Ca^{2+}. Compression rate is 1.9 $Å^2$ $molecule^{-1}$ min^{-1}. (b) Observed mean molecular areas as a function of subphase Ca^{2+} concentration at different surface pressures. The data are obtained from isotherms in (a).

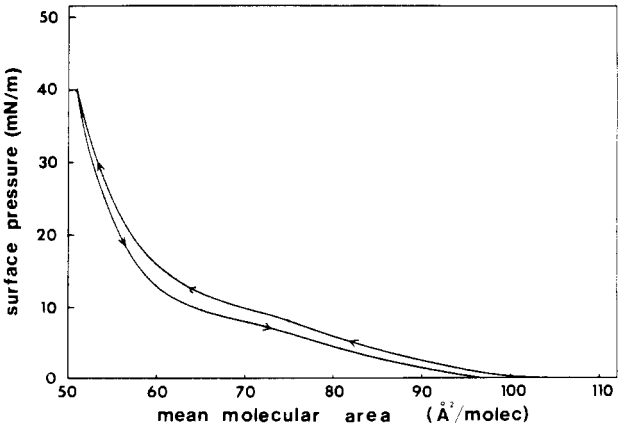

FIGURE 8: Compression–relaxation cycle for a DPPC/PPHPA (80:20) film over a subphase containing 5 mM $CaCl_2$. Compression rate is 1.9 $Å^2$ $molecule^{-1}$ min^{-1}.

At surface pressures higher than 10 mN m^{-1} mixing of the PC and PA phases occurred. This was more pronounced at 1 mM Ca^{2+} than at 30 mM Ca^{2+}. Due to the strong binding of Ca^{2+} to PA it is conceivable to assume that PPHPA in the presence of Ca^{2+} is in the condensed phase also at very low

surface pressures. As DPPC at low surface pressures is in the fluid state this would favor phase separation. As the surface pressure is increased, the electrostatic energy between charged PA head groups increases due to decreased area per lipid polar head group. In addition, at surface pressures above 10 mN m^{-1} DPPC is also in the condensed phase, and thus in order to decrease the electrostatic energy, mixing of PC with PA occurs. At 30 mM Ca^{2+} due to additional binding of Ca^{2+} the PA lattice is tightly held together with PA being effectively screened. Thus the mixing of the phases remains incomplete. Upon decompression of the film the decrease in the electrostatic energy and the melting of DPPC lead to phase separation. The melting of DPPC "in" the PA lattice results now in different surface textures than before the compression of the film (Figure 3e–g).

The most dramatic effect due to the inclusion of cholesterol into PC/PA monolayers in the presence of Ca^{2+} was the decrease in the size of the PA domains. Compared to the effects produced by only trace amounts of cholesterol in DPPC monolayers (Weis & McConnell, 1985) higher amounts of cholesterol were required in the present study. This is likely to indicate that electrostatic forces involved in Ca^{2+}-induced phase separation are stronger than the interactions involved in the phase transition of DPPC (Keller et al., 1986). However, the explanation (Weis & McConnell, 1985; Keller et al., 1986) that cholesterol accommodates at the fluid–solid interfaces and decreases the line tension is in accordance with the observed decrease in the domain sizes (i.e., an increase in the length of the phase boundary). At 50 mol % cholesterol no phase separation could be detected. It is possible that the size of the separated phases decreases beyond the resolution of our microscopy system. It has also been shown that cholesterol inhibits the Ca^{2+}-induced lateral segregation in both PC/PS and PE/PS membranes (Tilcock et al., 1984). Also, the decrease observed in the surface pressure value at which phase separation disappeared in the presence of 10 and 30 mol % cholesterol could indicate the absence of phase separation in films containing 50 mol % cholesterol.

Direct visualization of the phospholipid lateral phase separations gives fascinating possibilities to study membranes. Valuable information concerning the effects of various lipid compositions, different cations, proteins, etc. on the lateral distribution of phospholipids can be obtained. The size of the observed segregated phases is rather large compared to cellular scale. However, local variations in Ca^{2+} concentration and, in particular, the presence of cholesterol bring it closer to the dimensions of biological systems. In addition, the effect of cholesterol makes it possible to control the size of segregated phases when technical applications of lipid films are considered.

ACKNOWLEDGMENTS

We are grateful to V. Virta and L. Inkinen for their help in the construction of the equipment and to M. Nissinen for her skillful technical assistance.

Registry No. DPPC, 2644-64-6; Ca, 7440-70-2; dipalmitoylphosphatidic acid, 19698-29-4.

REFERENCES

Birrell, G. B., & Griffith, O. H. (1976) *Biochemistry 15*, 2925–2929

Förster, Th. (1969) *Angew. Chem. 81*, 364–374.

Gad, A. E. (1983) *Biochim. Biophys. Acta 728*, 377–382.

Gad, A. E., Silver, B. L., & Eytan, G. D. (1982) *Biochim. Biophys. Acta 690*, 124–132.

Galla, H.-J., & Sackmann, E. (1975) *Biochim. Biophys. Acta 401*, 509–529.

Galla, H.-J., & Hartman, W. (1980) *Chem. Phys. Lipids 27*, 199–219.

Graham, I., Gagné, J., & Silvius, J. R. (1985) *Biochemistry 24*, 7123–7131.

Haverstick, D. M., & Glaser, M. (1987) *Proc. Natl. Acad. Sci. U.S.A. 84*, 4475–4479.

Hresko, R. C., Sugâr, I. P., Barenholz, Y., & Thompson, T. E. (1986) *Biochemistry 25*, 3818–3823.

Hresko, R. C., Sugâr, I. P., Barenholz, Y., & Thompson, T. E. (1987) *Biophys. J. 51*, 725–733.

Ito, T., & Ohnishi, S.-I. (1974) *Biochim. Biophys. Acta 352*, 29–37.

Jacobson, K., & Papahadjopoulos, D. (1975) *Biochemistry 14*, 152–161.

Keller, D. J., McConnell, H. M., & Moy, V. T. (1986) *J. Phys. Chem. 90*, 2311–2315.

Kinnunen, P. K. J., Virtanen, J. A., Tulkki, A.-P., Ahuja, R. C., & Möbius, D. (1986) *Thin Solid Films 132*, 193–203.

Kinnunen, P. K. J., Tulkki, A.-P., Lemmetyinen, H., Paakkola, J. K., & Virtanen, J. A. (1987) *Chem. Phys. Lett. 136*, 539–545.

Kleeman, W., & McConnell, H. M. (1976) *Biochim. Biophys. Acta 419*, 206–222.

Kouaouci, R., Silvius, J. R., Graham, I., & Pézolet, M. (1985) *Biochemistry 24*, 7132–7140.

Leventis, R., Gagné, J., Fuller, N., Rand, R. P., & Silvius, J. R. (1986) *Biochemistry 25*, 6978–6987.

Linden, C. D., Wright, K. L., McConnell, H. M., & Fox, C. F. (1973) *Proc. Natl. Acad. Sci. U.S.A. 70*, 2271–2275.

Lösche, H., & Möhwald, H. (1984a) *Colloids Surf. 10*, 217–224.

Lösche, M., & Möhwald, H. (1984b) *Eur. Biophys. J. 11*, 35–42.

Marsh, D., Watts, A., & Knowles, P. F. (1976) *Biochemistry 15*, 3570–3578.

McConnell, H. M., Tamm, L. K., & Weis, R. M. (1984) *Proc. Natl. Acad. Sci. U.S.A. 81*, 3249–3253.

Mustonen, P., Virtanen, J. A., Somerharju, P. J., & Kinnunen, P. K. J. (1987) *Biochemistry 26*, 2991–2997.

Papahadjopoulos, D., Jacobson, K., Nir, S., & Isac, T. (1973) *Biochim. Biophys. Acta 311*, 330–348.

Papahadjopoulos, D., Vail, W. J., Pangborn, W. A., & Poste, G. (1976) *Biochim. Biophys. Acta 448*, 265–283.

Parente, R. A., & Lentz, B. R. (1986) *Biochemistry 25*, 1021–1026.

Peters, R., & Beck, K. (1983) *Proc. Natl. Acad. Sci. U.S.A. 80*, 7183–7187.

Silvius, J. R., & Gagné, J. (1984) *Biochemistry 23*, 3241–3247.

Somerharju, P. J., Virtanen, J. A., Eklund, K. K., Vainio, P., & Kinnunen, P. K. J. (1985) *Biochemistry 24*, 2773–2781.

Thuren, T., Vainio, P., Virtanen, J. A., Somerharju, P., Blomqvist, K., & Kinnunen, P. K. J. (1984) *Biochemistry 23*, 5129–5134.

Thuren, T., Virtanen, J. A., & Kinnunen, P. K. J. (1986) *Chem. Phys. Lipids 41*, 329–334.

Tilcock, S. P. C., Bally, M. B., Farren, S. B., Cullis, P. R., & Gruner, S. M. (1984) *Biochemistry 23*, 2696–2703.

van Dijck, P. W. M., De Kruijff, B., Verkleij, A. J., van Deenen, L. L. M., & De Gier, J. (1978) *Biochim. Biophys. Acta 512*, 84–96.

Weis, R. M., & McConnell, H. M. (1984) *Nature (London) 310*, 47–49.

Weis, R. M., & McConnell, H. M. (1985) *J. Phys. Chem. 89*, 4453–4459.